Contribution from the Department of Synthetic Chemistry, Faculty of Engineering, Kumamoto University, Kurokami, Kumamoto 860, Japan, and Institute for Molecular Science, Myodaiji, Okazaki 444, Japan

Comparison of Electronic Structure, Stereochemistry, and Coordinate Bonds between Ni(0)-SO_2 Complexes and Nonmetal SO_2 Complexes. An MO Study

Shigeyoshi Sakaki,*[1a] Hiroyuki Sato,[1a] Yukari Imai,[1a] Keiji Morokuma,[1b] and Katsutoshi Ohkubo[1a]

Received October 26, 1984

Several SO_2 complexes, $Ni(PH_3)_3(SO_2)$, $Ni(PH_3)_2(SO_2)$, $(NH_3)(SO_2)$, $N(CH_3)_3(SO_2)$, $(CN^-)(SO_2)$ (N coordinating with S), and $(NC^-)(SO_2)$ (C coordinating with S), were investigated with the ab initio MO method to shed some light on the difference in coordinate bond nature and stereochemistry (η^1-coplanar, η^1-pyramid, or η^2-SO coordination of SO_2) between the Ni(0)-SO_2 and nonmetal SO_2 complexes. Nonmetal complexes take the η^1-pyramid SO_2 coordination mode to maximize the overlap between the LUMO (π^*) of SO_2 and the lone pair of the Lewis base ($N(CH_3)_3$, NH_3, CN^-), and to minimize the exchange repulsion between the lone-pair orbitals of SO_2 and the Lewis base. Though $Ni(PH_3)_3(SO_2)$ is isolobal with $N(CH_3)_3(SO_2)$, the former takes the η^1-coplanar coordination mode of SO_2, due to the presence of the occupied d_π orbital at high energy levels and the bulky PH_3 ligands. η^2-SO coordination is often possible in transition-metal complexes, for the d_π orbital can give π-back-donation with the SO_2 π^* orbital. On the other hand, this coordination mode is difficult in nonmetal SO_2 complexes, because of the absence of such a π-donor orbital. Compared with nonmetal SO_2 complexes, the characteristic features of transition-metal complexes are deduced to come from the presence of the high-lying occupied Ni d_π orbital, the low-lying unoccupied Ni 4s orbital, and the bulky PH_3 ligands.

Introduction

Transition-metal complexes have received much attention in the last decade, because of their various stereochemistries, notable reactivity, and catalytic abilities.[2] On the other hand, nonmetal charge-transfer(CT) complexes, which possess a coordinate bond similar to that of transition-metal complexes, seldom show such interesting features. Though many MO studies of transition-metal complexes have been carried out to investigate their stereochemistry, coordinate bond nature, and reactivity,[3] few studies have been presented to make clear what factors lead to the above described difference between nonmetal CT complexes and transition-metal complexes and how transition-metal complexes can be characterized in comparison with nonmetal CT complexes.

Meanwhile, many SO_2 complexes, including nonmetal CT complexes and transition-metal complexes, have been synthesized, and they interestingly exhibit various coordination modes with SO_2;[4-14] for example, four kinds of coordination modes, η^1-coplanar, η^1-pyramid, η^2-SO side-on, and η^1-O end-on, are reported as shown in Chart I, and these coordination modes are considered to be sensitive to the electronic structure of SO_2 complexes.[7h,8,9] Another interesting point is also noted; it is difficult to find a molecule that can form both transition-metal complexes and nonmetal CT complexes, but SO_2 is one ot these rare molecules.[12,14] So, we can compare coordinate bond nature and electronic structure between nonmetal SO_2 complexes and transition-metal SO_2 complexes and investigate characteristic features of transition-metal complexes through such a comparison. Nevertheless, only a few MO studies of SO_2 complexes have been reported. To our knowledge, four ab initio MO studies of amine-SO_2 and HF-SO_2 complexes[15-17] and two semiempirical MO studies of Ir(I)-SO_2 and SO_2-quinol complexes[18] have been presented, but theoretical comparisons between nonmetal SO_2 complexes and transition-metal SO_2 complexes have not been carried out.

Chart I

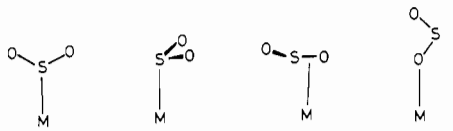

In this work, several SO_2 complexes, $N(CH_3)_3(SO_2)$, $(NH_3)(SO_2)$, $(CN^-)(SO_2)$ (N coordinating with S), $(NC^-)(SO_2)$ (C coordinating with S), $Ni(PH_3)_3(SO_2)$, and $Ni(PH_3)_2(SO_2)$, are investigated with ab initio MO method and energy decomposition analysis of interaction. These SO_2 complexes are chosen here for the following reasons: (1) Kollman has proposed in his ab initio MO study that electrostatic interaction is most important in $N(CH_3)_3(SO_2)$.[16] If so, the binding energy (BE) is expected to be proportional to the electrostatic interaction. Thus, a comparison of a series of nonmetal SO_2 complexes would give some information about the contribution of electrostatic interaction and the coordinate bond nature of nonmetal SO_2 complexes. (2) In the previous ab initio MO study of $N(CH_3)_3(SO_2)$,[16] the N-S distance was calculated to be too long. Therefore, it is worth reexamining the N-S distance with a better basis set. (3) $Ni(PH_3)_3$ has an occupied d_σ orbital at a high energy level, and $N(CH_3)_3$ also has a lone-pair orbital. Thus, we can consider that $Ni(PR_3)_3$ is isolobal

(1) (a) Kumamoto University. (b) Institute for Molecular Science.
(2) For example: Negishi, E. "Organometallics in Organic Synthesis"; Wiley: New York, 1980; Vol. 1. Wender, I.; Pino, P. "Organic Syntheses via Metal Carbonyls"; Wiley: New York, 1977. Kochi, J. K. "Organometallic Mechanisms and Catalysis"; Academic Press: New York, 1978. Henrici-Olivé, G.; Olivé, S. "Coordination and Catalysis"; Verlag Chemie: Weinheim, West Germany, 1977.
(3) For example: Steigerwald, M. L.; Goddard, W. A., III. *J. Am. Chem. Soc.* **1984**, *106*, 308. Noell, J. O.; Hay, P. J. *Ibid.* **1982**, *104*, 4578. Strich, A.; Veillard, A. *Nouv. J. Chim.* **1983**, *7*, 347. Nakatsuji, H.; Ushio, J.; Han, S.; Yonezawa, T. *J. Am. Chem. Soc.* **1983**, *105*, 426. Mealli, C.; Hoffmann, R.; Stockis, A. *Inorg. Chem.* **1984**, *23*, 56.
(4) Ryan, R. R.; Kubas, G. J.; Moody, D. C.; Eller, P. G. *Struct. Bonding (Berlin)* **1981**, *46*, 47.
(5) (a) La Placa, S. J.; Ibers, J. A. *Inorg. Chem.* **1966**, *3*, 405. (b) Muir, K. W.; Ibers, J. A. *Ibid.* **1969**, *8*, 1921. (c) Wilson, R. D.; Ibers, J. A. *Ibid.* **1978**, *17*, 2134.
(6) Dapporto, P.; Midollini, S.; Orlandini, A.; Sacconi, L. *Inorg. Chem.* **1976**, *15*, 2768.
(7) (a) Eller, P. G.; Ryan, R. R.; Moody, D. C. *Inorg. Chem.* **1976**, *15*, 2442. (b) Moody, D. C.; Ryan, R. R. *Ibid.* **1977**, *16*, 1052. (c) Eller, P. G.; Kubas, G. J.; Ryan, R. R. *Ibid.* **1977**, *16*, 2454. (d) Moody, D. C.; Ryan, R. R. *Ibid.* **1977**, *16*, 2473. (e) Moody, D. C.; Ryan, R. R. *Ibid.* **1979**, *18*, 223. (f) Moody, D. C.; Ryan, R. R.; Larson, A. C. *Ibid.* **1979**, *18*, 227. (g) Eller, P. G.; Ryan, R. R. *Ibid.* **1980**, *19*, 142. (h) Kubas, G. J.; Ryan, R. R.; McCarty, *Ibid.* **1980**, *19*, 3003. (i) Kubas, G. J.; Ryan, R. R. *Inorg. Chim. Acta* **1981**, *47*, 131. (j) Kubas, G. J.; Jarvinen, G. D.; Ryan, R. R. *J. Am. Chem. Soc.* **1983**, *105*, 1883. (k) Ritchey, J. M.; Moody, D. C.; Ryan, R. R. *Inorg. Chem.* **1983**, *22*, 2276.
(8) Johnson, D. A.; Dew, V. C. *Inorg. Chem.* **1979**, *18*, 3273.
(9) Kubas, G. J. *Inorg. Chem.* **1979**, *18*, 182 and references cited therein.
(10) Vasapollo, G.; Giannoccaro, P.; Nobile, C. F.; Sacco, A. *Inorg. Chim. Acta* **1981**, *48*, 125.
(11) Bell, L. K.; Mingos, D. M. P. *J. Chem. Soc., Dalton Trans.* **1982**, 673.
(12) (a) Christian, S. D.; Grundnes, J. *Nature (London)* **1967**, *214*, 1111. (b) Van der Helm, D.; Childs, J. D.; Christian, S. D. *J. Chem. Soc. D* **1969**, 887. (c) Childs, J. D.; Van der Helm, D; Christian, S. D. *Inorg. Chem.* **1975**, *14*, 1386. (d) Grundnes, J.; Christian, S. D. *J. Am. Soc.* **1968**, *90*, 2239.
(13) Moore, J. W.; Baird, H. W.; Miller, H. B. *J. Am. Chem. Soc.* **1968**, *90*, 1358.
(14) Eller, P. G.; Kubas, G. J. *Inorg. Chem.* **1978**, *17*, 894.
(15) Lucchese, R. R.; Haber, K.; Schaefer, H. F., III. *J. Am. Chem. Soc.* **1976**, *98*, 7617.
(16) (a) Kollman, P. A. *J. Am. Chem. Soc.* **1977**, *99*, 4875. (b) Douglas, J. E.; Kollman, P. A. *Ibid.* **1978**, *100*, 5226.
(17) (a) Pullman, A.; Bethod, H. *Chem. Phys. Lett.* **1981**, *81*, 195. (b) Friedlander, M. E.; Howell, J. M.; Sapse, A.-M. *Inorg. Chem.* **1983**, *22*, 100.
(18) (a) Ryan, R. R.; Eller, P. G. *Inorg. Chem.* **1976**, *15*, 494. (b) Tse, J. S.; Ripmeester, J. A. *J. Phys. Chem.* **1983**, *87*, 1708.

0020-1669/85/1324-4538$01.50/0

with $N(CH_3)_3$. However, $Ni(PR_3)_3(SO_2)$ takes the η^1-coplanar SO_2 coordination mode,[6,7e] unlike $N(CH_3)_3(SO_2)$, which possesses the η^1-pyramid SO_2 coordination mode.[12] It is interesting to investigate why $Ni(PH_3)_3(SO_2)$ takes the η^1-coplanar structure but $N(CH_3)_3(SO_2)$ takes the η^1-pyramid structure. (4) The η^2-SO coordination mode has been found in transition-metal SO_2 complexes[5c,7d,f,h] but never in nonmetal SO_2 complexes. Models of η^2-SO coordinate complexes, $Ni(PH_3)_2(\eta^2\text{-}SO_2)$ and $N(CH_3)_3(\eta^2\text{-}SO_2)$, were examined to show what factors determine the stability of the η^2-SO coordination complexes. Through this investigation, the authors attempt to make clear characteristic features of transition-metal complexes in comparison with nonmetal CT complexes.

Computational Method

Ab initio SCF–MO calculations were performed for the closed-shell (singlet) state.[19] Although $^3D(3d^94s^1)$, $^3F(3d^84s^2)$, and $^1S(3d^{10})$ lie energetically very close to each other in the free Ni atom, $Ni(PR_3)_3(SO_2)$ is a diamagnetic compound[6] and its ground state is considered to be a singlet. When stabilizing ligands such as phosphines and carbonyls coordinate with Ni(0), the Ni(0) complex would become a singlet, as discussed previously.[20] The essence of the discussion is that the stabilizing ligand would make the $3d^{10}$ configuration more stable than the $3d^94s$ and $3d^84s^2$ configurations.

The 3-21G basis set was used in geometry optimization of nonmetal SO_2 complexes,[21a] and the better basis set, 6-31G,[21b,c] was also used to discuss the coordinate bond and electronic structure of nonmetal SO_2 complexes, where d-polarization functions (without a spherical d function; $\zeta_{3d} = 0.8$ for N and $\zeta_{3d} = 0.65$ for S)[22] were included on S of SO_2 and N of NH_3 and $N(CH_3)_3$. In geometry optimization of Ni complexes, the relatively small [4s 3p 2d] contracted set[23] and the usual STO-3G* set were used for Ni and ligand atoms, respectively, where the d-polarization functions were included on only the S atom and the Ni [4s 3p 2d] set was contracted from the (11s 7p 5d) primitive set. To discuss bonding nature, MO calculations were carried out with a better basis set; for Ni, the double-ζ quality [5s 4p 2d] basis set, contracted from the (13s 9p 6d) primitives,[25] was employed, and for ligand atoms, the 3-21G set was used with d-polarization functions (excluding a spherical d function; $\zeta_{3d} = 0.65$) only on the S atom.

The energy decomposition analysis (EDA) was carried out in order to investigate the electronic structure and coordinate bond nature in detail.[26] Here, the binding energy (BE) is defined as the stabilization of a total complex $ML_n{\cdot}SO_2$ relative to ML_n and SO_2 fragments, taking the respective equilibrium structure, and it can be represented as

$$BE = INT + DEF$$

$$INT = E_t(ML_n{\cdot}SO_2) - E_t(ML_n)_{dis} - E_t(SO_2)_{dis}$$

$$DEF = [E_t(ML_n)_{dis} - E_t(ML_n)_{eq}] + [E_t(SO_2)_{dis} - E_t(SO_2)_{eq}]$$

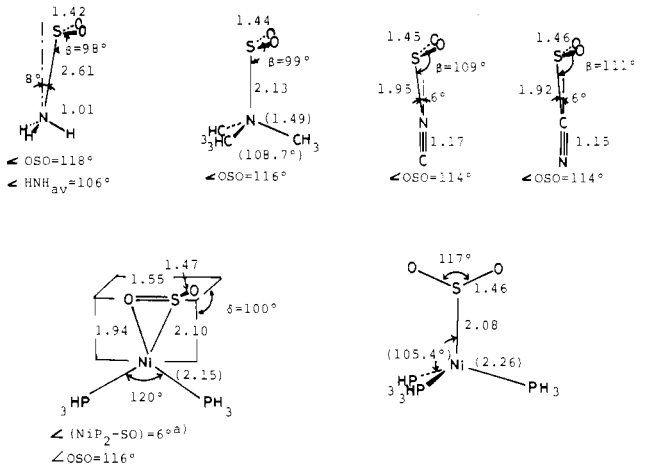

Figure 1. Optimized structures of examined SO_2 complexes: β, angle between the SO_2 plane and the SO_2 coordinate bond; δ, angle between the SO_2 plane and the Ni–S–O plane.

where DEF (deformation energy)[26d] is the destabilization energy to deform ML_n and SO_2 from their equilibrium structures to the distorted structures that are taken in the complex and INT (interaction energy) is the stabilization energy of the total complex relative to that of the deformed ML_n and SO_2. INT is further divided into various chemically meaningful terms

$$INT = ES + EX + MSCTPLX + SMCTPLX + R$$

ES and EX are electrostatic interaction and exchange repulsion interaction, respectively. MSCTPLX represents the charge transfer from ML_n to SO_2, the SO_2 polarization, and their coupling term. SMCTPLX is the charge-transfer term from SO_2 to ML_n, the ML_n polarization, and their coupling term. R is the remaining higher order coupling term. The details of the EDA scheme have been described elsewhere.[26]

Geometry Optimization. Geometries of nonmetal SO_2 complexes were fully optimized by using the energy gradient technique, except for $N(CH_3)_3(SO_2)$. In $N(CH_3)_3(SO_2)$ and $Ni(PH_3)_3(SO_2)$, the Ni–S, N–S, and S–O distances, the OSO angle, and the angle between the SO_2 plane and the Ni–S or N–S bond (hereafter, abbreviated as the β angle; see Figure 1) were optimized by a parabolic fit of total energy. The geometries of $N(CH_3)_3$ and $Ni(PH_3)_3$, taken from the similar SO_2 complexes,[27] were fixed during optimization, and the S atom was assumed to be placed on the C_{3v} axes of $N(CH_3)_3$ and $Ni(PH_3)_3$. In $N(CH_3)_3(SO_2)$, the SO_2 ligand was placed so as to be bisected by an S–N–CH_3 plane, in accord with the experimental structure of this compound (see Figure 1).[12b] In $Ni(PH_3)_3(SO_2)$, the SO_2 ligand was assumed to be symmetric with respect to the Ni–S bond. The β angle was optimized, and as a result, the coplanar structure ($\beta = 180°$) was found to be the most stable. Since the rotation of SO_2 around the coordinate bond was calculated to give little energy change, the SO_2 plane was placed to be eclipsed with a Ni–PH_3 bond; the experimental structure of $Ni(PPh_3)_3(SO_2)$ has a similar orientation of SO_2.[7e] In the η^1-pyramidal $Ni(PH_3)_3(SO_2)$, the β angle was assumed to be 90°, a rough model to be compared with the coplanar structure.

$Ni(PH_3)_2(\eta^2\text{-}SO_2)$ was examined as a model complex of the η^2-SO coordination, where the geometry of $Ni(PH_3)_2$ was taken from similar complexes[28] and fixed during optimization. On the assumption that the coordinating S=O bond is perpendicular to the C_{2v} axis of $Ni(PH_3)_2$, the following geometrical parameters were optimized: the S=O distance, the OSO angle, the distance between Ni and the coordinating S=O bond, the angle between the SO_2 plane and the Ni–S–O plane (hereafter, abbreviated as δ; see Figure 1), the coordinating S=O rotation around the C_{2v} axis of $Ni(PH_3)_2$, and the slide movement of the coordinating S=O bond (this movement takes account of the difference in the Ni–S and Ni–O distances). The η^2-coordinating $N(CH_3)_3(\eta^2\text{-}SO_2)$ does not even correspond to a local minimum and isomerizes to its η^1-S pyramid structure with no barrier, as described later. Therefore, the model η^2-SO coordinating complex, $N(CH_3)_3(\eta^2\text{-}SO_2)$, was assumed to take the fol-

(19) The program used for MO calculations was IMSPACK (Morokuma, K.; Kato, S.; Kitaura, K.; Ohmine, I.; Sakai, S.; Obara, S. IMS Computer Center Program Library, Institute for Molecular Science, 1980; No. 0372), consisting of GAUSSIAN 70, HONDO, and many other routines.
(20) Sakaki, S.; Kitaura, K.; Morokuma, K. *Inorg. Chem.* **1982**, *21*, 760.
(21) (a) Binkley, J. S.; Pople, J. A.; Hehre, W. J. *J. Am. Chem. Soc.* **1980**, *102*, 939. Gordon, M. S.; Binkley, J. S.; Pople, J. A.; Pietro, W. J.; Hehre, W. J. *Ibid.* **1982**, *104*, 2297. (b) Hehre, W. J.; Ditchfield, R.; Pople, J. A. *J. Chem. Phys.* **1972**, *56*, 2257. (c) Francl, M. M.; Pietro, W. J.; Hehre, W. J.; Binkley, J. S.; Gordon, M. S.; DeFrees, D. J.; Pople, J. A. *Ibid.* **1982**, *77*, 3654.
(22) The exponents of d-polarization functions are taken from ref 21c and: Hariharan, P. C.; Pople, J. A. *Mol. Phys.* **1974**, *27*, 209. The spherical d function was excluded in all of our MO calculations of transition metal complexes. Therefore, the spherical d function was also excluded here even in calculations of nonmetal SO_2 complexes, to compare the nonmetal complex with Ni(0)–SO_2 complexes, though six components of d functions are used in usual 6-31G* and 3-21G* calculations.
(23) Roos, B.; Veillard, A.; Vinot, G. *Theor. Chim. Acta* **1971**, *20*, 1. Hay, P. J. *J. Chem. Phys.* **1977**, *66*, 4377. $\zeta_{4s} = 0.20$ and $\zeta_{4p} = 0.25$ were added into the basis set employed.
(24) Collins, J. B.; Schleyer, P. v. R.; Binkley, J. S.; Pople, J. A. *J. Chem. Phys.* **1976**, *64*, 5142.
(25) Hyla-Kryspin, I.; Demuynck, J.; Strich, A.; Bénard, M. *J. Chem. Phys.* **1981**, *75*, 3954. The following modifications were carried out: for the s orbital, $\zeta = 0.047\,791$ was deleted but $\zeta = 0.30$ was added; for the p orbital, $\zeta = 0.45$ and 0.20 were added; for the d orbital, $\zeta = 0.11$ was added. Then, (13s 9p 6d) was contracted [72211/5211/51] with a decrease in the exponents.
(26) (a) Morokuma, K. *Acc. Chem. Res.* **1977**, *10*, 294. (b) Kitaura, K.; Morokuma, K. *Int. J. Quantum Chem.* **1976**, *10*, 325. (c) Kitaura, K.; Sakaki, S.; Morokuma, K. *Inorg. Chem.* **1981**, *20*, 2292. (d) The DEF value of the metal fragment is not considered here.
(27) The geometry of $N(CH_3)_3$ was taken from the experimental structure of $N(CH_3)_3(SO_2)$.[12b] The geometry of $Ni(PH_3)_3$ was taken from the experimental structure of $Ni(PPh_3)_3(SO_2)$.[7e]
(28) The geometry of the $Ni(PH_3)_2$ part was taken from the experimental structure of $Ni(PPh_3)_2(C_2H_4)$. Joly, P. W.; Wilke, G. "The Organic Chemistry of Nickel"; Academic Press: New York, 1978; Vol. I, Chapter V.

Table I. Comparisons between Optimized Geometrical Parameters and Observed Ones[a]

	optimized	obsd	
	$N(CH_3)_3(SO_2)$	$N(CH_3)_3(SO_2)$[12b]	$(CH_3)_2NC_6H_4N(CH_3)_2(SO_2)_2$[12c]
N–S	2.13	2.06	2.340
S–O	1.44	1.3965 (av)	1.434
β[b]	99	112	105.2
∠OSO	116	114.8	113.5

	optimized	obsd	
	$Ni(PH_3)_3(SO_2)$	$Ni(P_3)(SO_2)$	$Ni(PPh_3)_3(SO_2)$[7e]
Ni–S	2.08	2.013	2.038
S–O	1.46	1.365	1.4475
β[b]	180	180	166.9
∠OSO	117	109.1	113.4

	optimized	obsd			
		$Mo(CO)_3(NN)(\eta^2\text{-}SO_2)$[7f]		$RuCl(NO)(PPh_3)_2(\eta^2\text{-}SO_2)$[5c]	$Rh(NO)(PPh_3)_2(\eta^2\text{-}SO_2)$[7d]
	$Ni(PH_3)_2(\eta^2\text{-}SO_2)$	NN = phen	NN = bpy		
M–S	2.10	2.532	2.496	2.337	2.326
$M–O_c$[c]	1.94	2.223	2.111	2.144	2.342
$S–O_c$	1.55	1.468	1.550	1.504	1.493
$S–O_t$[c]	1.47	1.435	1.452	1.459	1.430
∠OSO	116	117.3	113.4	113.7	115.1
δ[d]	100	108.1	103.4	110.3	100.3

	optimized SO_2		obsd
	3-21G[e]	STO-3G*[24]	SO_2[f]
S–O	1.417	1.446	1.4308
∠OSO	119	119.88	119.32

[a] Distances in Å and angles in deg. [b] The angle between the SO_2 plane and the Ni–S bond (see Figure 1). [c] O_c and O_t represent the coordinating O atom of SO_2 and the terminal O atom of SO_2, respectively. [d] The angle between the SO_2 plane and the MSO_c plane (see Figure 1). [e] Five components of d-type-polarization functions are included on the S atom (see text and ref 22). [f] Herzberg, G. "Molecular Spectra and Molecular Structure"; Van Nostrand: Princeton, NJ, 1967; Vol. I, p 605.

lowing structure; the structure of SO_2 was taken to be the optimized structure of free SO_2, the coordinating S=O bond was placed perpendicular to the C_{3v} axis of $N(CH_3)_3$, and the δ angle was equal to that of $Ni(PH_3)_2(\eta^2\text{-}SO_2)$.

Results and Discussion

Optimized Structures. Optimized structures are displayed schematically in Figure 1, and several important geometrical parameters are compared with the corresponding experimental values in Table I.

First, let us examine the optimized structure of nonmetal SO_2 complexes. All of the nonmetal SO_2 complexes studied take a η^1-pyramid structure, which agrees with the experiments.[7c,12] Though the N–S distance of $(NH_3)(SO_2)$ is calculated to be remarkably long, the calculated N–S distance of $N(CH_3)_3(SO_2)$ is much shorter than that of $(NH_3)(SO_2)$ and agrees well with the experimental N–S distance of this compound (see Table I).[12b] In the previous ab initio MO study of $N(CH_3)_3(SO_2)$, a rather long N–S distance (2.36 Å) was calculated,[16] where the β angle was not optimized but fixed to be 95° and the usual 4-31G basis set was used without d-polarization functions. In the present calculations, all the geometrical parameters including the β angle and the SO_2 geometry were optimized, and the d-polarization functions were included in the basis sets of S and N. These improvements would result in a good N–S distance; in particular, the optimization of β and the SO_2 geometry is important to get a good N–S distance, because the potential curve is very shallow with respect to the N–S distance, and furthermore the N–S distance is sensitive to the β value and SO_2 geometry. For example, N–S = 2.22 Å for assumed β = 96°, S=O 1.422 Å, and ∠OSO = 117.6°, but N–S = 2.13 Å after optimization of β and SO_2 geometry (β = 99°, S=O = 1.436 Å, and ∠OSO = 116.8°). The calculated coordinate bond of SO_2 becomes longer in the order $(NC^-)(SO_2) > (CN^-)(SO_2) > N(CH_3)_3(SO_2) >> (NH_3)(SO_2)$, suggesting that $(NH_3)(SO_2)$ is the weakest and that $(NC^-)(SO_2)$ is the strongest complex among the nonmetal SO_2 complexes examined.

The optimized structure of $Ni(PH_3)_3(SO_2)$ has the η^1-coplanar coordination of SO_2, in accord with the experimental structure of $Ni(P_3)(SO_2)$ (P_3 = tridentate chelate phosphine).[6] Furthermore, the optimized Ni–S and S–O distances and the OSO angle agree well with experimental values, as compared in Table I. The SO_2 rotation around the Ni–S bond gives little energy change, as described above. In fact, the SO_2 ligand is eclipsed with one $Ni–PPh_3$ bond in $Ni(PPh_3)_3(SO_2)$,[7e] but in $Ni(P_3)(SO_2)$, the SO_2 plane is placed to be perpendicular to one P–Ni–S plane.[6] Thus, the SO_2 orientation around the coordinate bond is considered to be very sensitive to the surrounding situation.

The model complex of η^2-SO coordination, $Ni(PH_3)_2(\eta^2\text{-}SO_2)$, shows several characteristic features found in η^2-SO coordinate complexes; for example, the Ni–S bond is longer than the Ni–O bond. Similar results have been found in some η^2-SO-coordinated complexes with only the exception of $Rh(NO)(PPh_3)_2(\eta^2\text{-}SO_2)$.[7d] The δ angle was optimized to be 100°. This value is in good agreement with experimental values, though the central metals are different (see Table I). These results have encouraged us to consider that this model complex, $Ni(PH_3)_2(\eta^2\text{-}SO_2)$, would offer information about the coordinate bond nature and the electronic structure of η^2-SO coordination.

Coordinate Bond and Stereochemistry of Nonmetal SO_2 Complexes. The SO_2 binding energy of $N(CH_3)_3(SO_2)$ was calculated to be 11.3 kcal/mol with the 6-31G set (d functions on S and N), as is shown in Table II, which agrees well with the experimental enthalpy for this complex formation (9.7 kcal/mol in the gas phase and 11.0 kcal/mol in heptane).[12a,d] In all of the complexes examined, ES interaction contributes most to the SO_2 coordination, as has been reported by Kollman.[16] However, the EX repulsion exceeds the ES stabilization, and the BSCTPLX interaction,[29] corresponding to the donation from the base to SO_2, is necessary for stable SO_2 coordination. The important role of this interaction is also suggested by the result of the electron distribution that Mulliken population of SO_2 is increased by the coordination and the quantity of the increased Mulliken population, Δq_{SO_2}, becomes

(29) SBCTPLX and BSCTPLX correspond to SMCTPLX and MSCTPLX of Ni(0)–SO_2 complexes, which are described in the Computational Method.

Table II. Energy Decomposition Analysis of Nonmetal SO_2 Complexes (kcal/mol)

	6-31G[a]				3-21G[a]		
	$(NC^-)(SO_2)$	$(CN^-)(SO_2)$	$N(CH_3)_3(SO_2)$	$(NH_3)(SO_2)$	$(NC^-)(SO_2)$	$(CN^-)(SO_2)$	$N(CH_3)_3(SO_2)$
r_{S-X}[d]	1.923[b] (2.183)[c]	1.948[b] (2.090)[c]	2.130	2.602[b] (2.114)[c]	1.923[b]	1.948[b]	2.13[b]
BE	−38.5 (−34.9)	−33.3 (−32.3)	−11.3	−7.9 (−1.3)	−38.2	−37.5	−15.7
DEF	4.0 (4.0)	1.5 (1.5)	0.4	0 (0)	0.6	2.3	0.9
INT	−42.5 (−38.9)	−34.8 (−33.7)	−11.7	−7.9 (−1.3)	−42.9	−39.7	−16.6
ES	−150.9 (−79.0)	−111.9 (−78.7)	−69.7	−19.9 (−70.1)	−149.6	−105.5	−57.9
EX	239.8 (108.7)	165.3 (108.7)	108.7	20.7 (108.7)	238.9	152.3	93.1
BSCTPLX	−110.2 (−56.9)	−71.0 (−48.0)	−34.7	−6.8 (−30.9)	−104.6	−67.0	−31.2
SBCTPLX	−16.7 (−8.9)	−18.2 (−12.3)	−12.8	−1.7 (−8.2)	−20.1	−16.7	−13.9
R	−4.5 (−2.8)	1.0 (0.6)	−3.2	−0.2 (−0.9)	−7.4	−2.8	−6.7
Δq_{SO_2}	0.423	0.273	0.169	0.048	0.317	0.275	0.159

[a] d-Polarization functions (without spherical d) are included on S and N for NH_3 and $N(CH_3)_3$ compounds. [b] The optimized structure. [c] The structure giving the same EX value as that of $N(CH_3)_3(SO_2)$ in which SO_2 is placed far away from the base without changes of orientation and its structure. [d] In Å.

large with increasing BE value (see Table II).

To investigate these complexes in detail, we compare the energy components at the same interfragment distance between the Lewis base and SO_2. As has been described previously,[20,30] the EX value is considered to be a measure of the interfragment distance, and these complexes are compared at the interfragment distance giving the standard EX value, which was taken somewhat arbitrarily to be the EX value of $N(CH_3)_3(SO_2)$, 108 kcal/mol. At this interfragment distance, all of the examined complexes receive similar ES and SBCTPLX (donation from SO_2 to the base)[29] stabilizations, as shown in Table II. It is noted that the BE and Δq_{SO_2} values decrease with decreasing BSCTPLX (donation from base to SO_2)[29] in the order $(NC^-)(SO_2) > (CN^-)(SO_2) > N(CH_3)_3(SO_2) > (NH_3)(SO_2)$. Consequently, it can be said that the relative stability of nonmetal SO_2 complex strongly depends on the BSCTPLX interaction. In other words, a stronger Lewis base, possessing a better donor ability, can form a more stable SO_2 coordinate bond.

Now, it is necessary to examine how energy components depend on basis sets, because the better 6-31G (with d functions on S) basis set was not used for ligand atoms of Ni complexes but the moderate 3-21G (with d functions on S) was used due to the large size of Ni(0)–SO_2 complexes. As shown in Table II, results calculated by using both the 6-31G and the 3-21G basis sets are almost the same in $(NC^-)(SO_2)$ and $(CN^-)(SO_2)$. In $N(CH_3)_3(SO_2)$, some differences are found between these two calculations, as follows: The 3-21G calculation gives the larger BE value than the 6-31G calculation does, perhaps due to the basis set superposition error. The 3-21G calculation also presents values less absolute for ES and EX than the 6-31G calculation, probably because of less accurate representation of core orbitals. However, the sum of ES and EX, corresponding to the static interaction, is almost the same in both the 6-31G and the 3-21G calculations. Furthermore, BSCTPLX and SBCTPLX contribute to the SO_2 coordination to a similar degree in both calculations. Also, both basis sets can offer similar results for the stereochemistry of nonmetal SO_2 complexes, as will be described later. Thus, even in $N(CH_3)_3(SO_2)$, the moderate 3-21G calculation seems sufficient enough to discuss qualitatively the coordinate bond nature and stereochemistry. A comparison between nonmetal SO_2 and Ni(0)–SO_2 complexes is carried out by using the 3-21G basis set for ligand atoms, in this work.

Now, we can investigate why the nonmetal SO_2 complexes examined take the η^1-pyramid coordination of SO_2 rather than the η^1-coplanar coordination mode. Figure 2 shows changes in INT and various energy components caused by the geometry change from the η^1-pyramid to η^1-coplanar coordination mode, in which only the β value was altered and the other geometrical parameters were fixed. For $N(CH_3)_3(SO_2)$, the solid lines represent the 3-21G calculation and the dashed lines the 6-31G calculation. Again, the 6-31G calculation gives larger absolute values for ES and EX than the 3-21G calculation does, but the

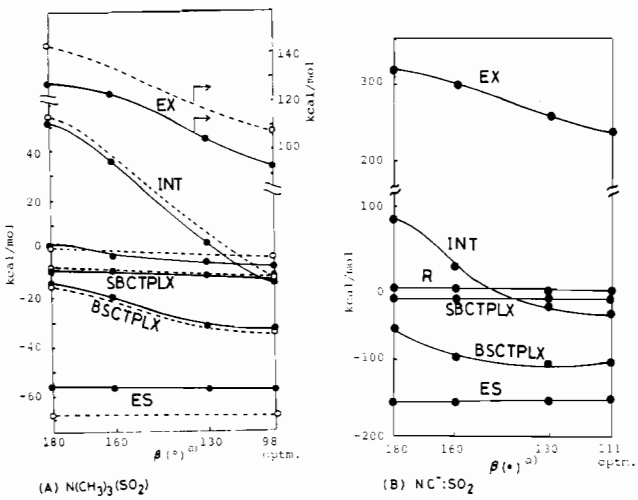

Figure 2. Changes in INT and various energy components, when going from the η^1-coplanar ($\beta = 180°$) to the η^1-pyramid structure. β is the angle between the SO_2 plane and the SO_2 coordinate bond (see Figure 1).

sum of ES and EX is not so much different between these two calculations. Furthermore, both calculations offer essentially the same energy changes in INT and energy components, when the coordination mode transforms from the η^1-pyramid to the η^1-coplanar structure. In $(NC^-)(SO_2)$ and $(CN^-)(SO_2)$, both basis sets give almost the same energy changes for the transformation of coordination mode; results of the 6-31G calculations are omitted in Figure 2 for simplicity. Then, we can see changes in energy components caused by the transformation of coordination mode. As shown in Figure 2, the EX repulsion increases and the BSCTPLX stabilization decreases, when the β value increases to 180° from its optimum angle. The other interactions, ES, SBCTPLX, and R, vary little during this geometry change. Consequently, INT becomes positive at $\beta = 180°$; i.e., the η^1-coplanar structure can not exist. Next, it should be investigated why the η^1-coplanar structure suffers from a large EX repulsion but receives a small BSCTPLX stabilization. Some orbital interactions, relating to these two interactions, are shown in Chart II. In the η^1-coplanar structure, the EX repulsion arises from the overlap of two occupied orbitals, lone-pair orbitals of SO_2 and $N(CH_3)_3$. In the η^1-pyramid structure, however, the SO_2 lone pair avoids the $N(CH_3)_3$ lone pair, leading to less EX repulsion than in the η^1-coplanar structure. A critical contrast is also found in the BSCTPLX interaction. The η^1-pyramid structure has good overlap between the lone-pair orbital of $N(CH_3)_3$ and the π^* orbital of SO_2, whereas the η^1-coplanar structure has little overlap between these two orbitals. Thus, these two interactions, EX and BSCTPLX, favor the η^1-pyramid structure but disfavor the η^1-coplanar structure. As a result, the η^1-pyramid coordination mode becomes the equilibrium structure of nonmetal SO_2 complexes.

Coordinate Bond Nature and Stereochemistry of $Ni(PH_3)_3(SO_2)$. In contrast with the nonmetal SO_2 complexes, $Ni(PH_3)_3(SO_2)$

(30) Sakaki, S.; Kitaura, K.; Morokuma, K.; Ohkubo, K. *Inorg. Chem.* **1983**, *22*, 104.

Chart II

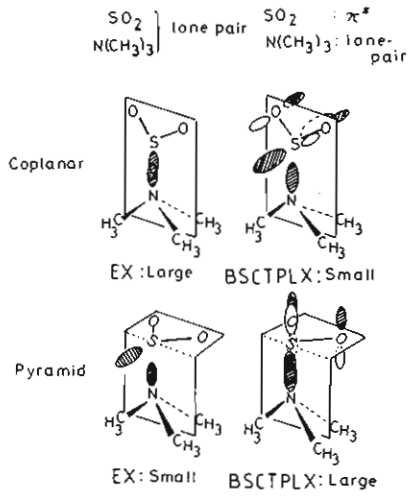

Table III. Energy Decomposition Analysis of $Ni(PH_3)_3(SO_2)$ and Comparison of $Ni(PH_3)_3(SO_2)$ with $N(CH_3)_3(SO_2)$ (kcal/mol)

	$Ni(PH_3)_3(SO_2)$		$N(CH_3)_3(SO_2)$	
	β^a = 180°	β = 90°	β = 99°	β = 180°
R_{S-Ni}[e]	2.08	2.08	2.130[b] (2.048)[c]	2.130
BE	−18.7	−17.3	−15.7 (−15.5)	53.4
DEF[d]	3.0	3.0	0.9 (0.9)	0.9
INT	−21.7	−20.3	−16.6 (−16.4)	52.5
ES	−83.1	−69.0	−57.9 (−74.1)	−56.6
EX	118.2	123.3	93.1 (123.3)	128.8
MSCTPLX	−28.4	−33.6	−31.2 (−39.5)	−13.4
SMCTPLX	−20.5	−19.7	−13.9 (−18.0)	−8.2
R	−7.8	−21.4	−6.7 (−8.1)	2.0

[a] See footnote *b* of Table I. [b] The optimized structure. [c] See footnote *c* of Table II. [d] The geometry of $Ni(PH_3)_3$ was fixed, like in our previous works.[20,30] [e] In Å.

takes η^1-coplanar coordination as its most stable structure, though the energy difference between the η^1-coplanar and the η^1-pyramid structures is very small (only 1.5 kcal/mol). This small energy difference seems to correspond with the experimental proposal that Ni(0)–SO_2 complexes are borderline cases between the η^1-coplanar and η^1-pyramid structures;[7e] in fact, $Ni(P_3)(SO_2)$ takes the η^1-coplanar structure,[6] but $Ni(PPh_3)_3(SO_2)$ is slightly distorted from the η^1-coplanar structure, where the SO_2 ligand is angled with the Ni–S bond by 166.9°.[7e]

First, the coordinate bond nature of $Ni(PH_3)_3(SO_2)$ will be examined. In a manner similar to that of the nonmetal SO_2 complexes, the ES interaction contributes most to the SO_2 coordination in both structures, but the EX repulsion exceeds the ES interaction, as shown in Table III. Thus, the charge-transfer interactions, MSCTPLX and SMCTPLX, are also important in $Ni(PH_3)_3(SO_2)$. Of these two interactions, the MSCTPLX stabilization is larger than the SMCTPLX stabilization. These interactions change Mulliken populations, as given in Table IV. The SO_2 ligand is negatively charged in both structures, according to the larger MSCTPLX interaction. The MSCTPLX interaction decreases the Ni d_{yz} orbital population in the η^1-coplanar structure and the Ni d_{z^2} orbital population in the η^1-pyramid structure. The SMCTPLX interaction increases the Ni sp orbital population in both structures. Thus, the Ni d_{yz} orbital participates in the MSCTPLX interaction of the η^1-coplanar structure, but the d_{z^2} orbital participates in the MSCTPLX of the η^1-pyramid structure. Ni sp orbitals contribute to the SMCTPLX interaction in both structures.

We will attempt to explain why the η^1-coplanar structure is more stable than the η^1-pyramid one in $Ni(PH_3)_3(SO_2)$. The η^1-pyramid structure of this complex suffers from larger EX repulsion than the η^1-coplanar structure, as shown in Table III. This feature is in critical contrast with the nonmetal SO_2 complexes discussed above; in the latter the η^1-coplanar structure suffers from a larger EX repulsion than the η^1-pyramid one. As shown in Chart III, the SO_2 lone-pair orbital overlaps with the occupied Ni d_{z^2} orbital to cause large four-electron destabilization (a part of EX repulsion) in the η^1-coplanar structure, whereas the steric repulsion between SO_2 and bulky PH_3 ligands (also another part of EX repulsion) is rather small. In the η^1-pyramid structure, the lone-pair orbital avoids the Ni d_{z^2} orbital but overlaps with the occupied Ni d_{yz} orbital to cause another type of four-electron destabilization. Furthermore, the steric repulsion between SO_2 and bulky PH_3 ligands is considerably larger in the η^1-pyramid than in the η^1-coplanar structure. Therefore, the overall EX repulsion of the η^1-pyramid structure is larger than that of the η^1-coplanar one. Another contrast is found in charge-transfer interaction; though the η^1-coplanar nonmetal SO_2 complexes receive much smaller BSCTPLX stabilization (about one-half) than the η^1-pyramid ones, the η^1-coplanar $Ni(PH_3)_3(SO_2)$ receives a moderately large MSCTPLX stabilization. This difference probably comes from the presence of the occupied Ni d_{yz} orbital, as follows. As shown in Chart III, the occupied Ni d_{z^2} orbital overlaps well with the SO_2 π^* orbital to form a strong Ni → SO_2 charge-transfer interaction in the η^1-pyramid structure, like the lone-pair orbital of nonmetal SO_2 complexes. Therefore, the d_{z^2} orbital population is decreased in the η^1-pyramid structure. In the η^1-coplanar structure, however, the d_{z^2} orbital cannot form such a Ni → SO_2 charge-transfer interaction, but the occupied Ni d_{yz} orbital can form the moderately strong Ni → SO_2

Table IV. Mulliken Population Analysis of $Ni(PH_3)_3(SO_2)$ and $N(CH_3)_3(SO_2)$

	tot	EX	MSCTPLX	SMCTPLX	*R*
		$Ni(PH_3)_3(SO_2)$ β = 180°			
Ni	0.217	−0.001	−0.125	0.229	0.114
sp	0.366	0.005	0	0.210	0.150
d	−0.149	−0.006	−0.125	0.018	0.036
d_{x^2}	0.042	0.017	0.003	0.026	−0.004
d_{y^2}	0.048	0.016	0.001	0.030	0.001
d_{z^2}	−0.068	−0.039	−0.024	−0.064	0.059
d_{yz}	−0.203	0	−0.073	−0.021	−0.109
PH_3	−0.088	0	−0.013	−0.047	−0.028
SO_2	0.046	0	0.162	−0.087	−0.029
		$Ni(PH_3)_3(SO_2)$ β = 90°			
Ni	0.153	0.001	−0.160	0.228	0.083
sp	0.379	0.004	−0.002	0.146	0.240
d	−0.226	−0.003	−0.158	0.082	−0.157
d_{x^2}	−0.070	0.012	−0.035	0.019	−0.065
d_{y^2}	0.007	0.012	0.020	0.032	−0.058
d_{z^2}	−0.261	−0.029	−0.082	−0.017	−0.132
d_{yz}	−0.043	0	−0.019	−0.008	−0.016
PH_3	−0.107	0	−0.008	−0.039	−0.060
SO_2	0.168	0	0.184	−0.114	0.098
		$N(CH_3)_3(SO_2)$ β = 90°			
N	0.142	−0.010	−0.132	−0.183	0.101
CH_3	−0.104	0.003	−0.008	−0.065	−0.034
SO_2	0.169	0	0.156	0.012	0.001

Chart III

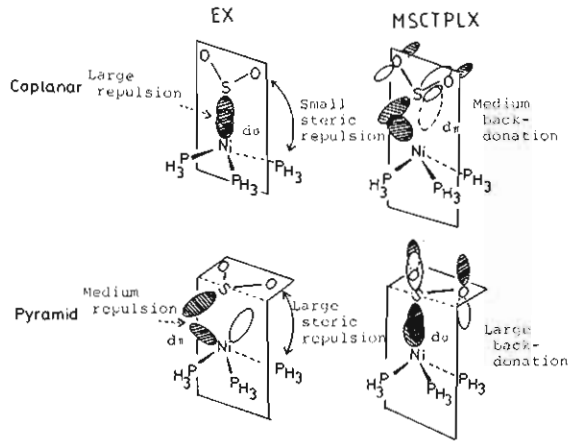

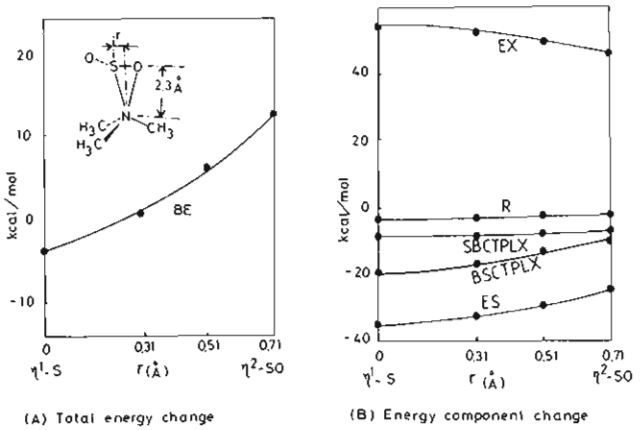

Figure 3. Total energy and energy component changes going from the η^2-SO coordination to the η^1-S coordination. The orientation and geometry of SO_2 was not altered.

charge-transfer interaction, as shown in Chart III. Actually, the Ni d_{yz} orbital population is decreased by the SO_2 coordination in the η^1-coplanar structure (see Table IV). On the other hand, the η^1-coplanar nonmetal SO_2 complex cannot form any effective base → SO_2 charge-transfer interaction, because Lewis bases do not have a good π-donating orbital. In conclusion, $Ni(PH_3)_3(SO_2)$ has bulky PH_3 ligands and the occupied Ni d_{yz} orbital, which leads to the large EX repulsion in the η^1-pyramid structure and the moderate MSCTPLX stabilization in the η^1-coplanar one. As a result, the η^1-coplanar structure is the most stable in $Ni(PH_3)_3(SO_2)$.

Now, a comparison between $Ni(PH_3)_3(SO_2)$ and $N(CH_3)_3(SO_2)$ will be mainly carried out for the η^1-pyramid structure, because the η^1-coplanar $N(CH_3)_3(SO_2)$ is very unstable and would possess an unreasonable SO_2 coordinate bond. As shown in Table III, $N(CH_3)_3(SO_2)$ has slightly larger ES and BSCTPLX stabilization than $Ni(PH_3)_3(SO_2)$ at the interfragment distance giving the same EX value, but the SMCTPLX stabilization of $Ni(PH_3)_3(SO_2)$ is slightly larger than that of $N(CH_3)_3(SO_2)$, perhaps due to the presence of the acceptor Ni 4sp orbitals. A difference is also found at the higher order *R* term; $Ni(PH_3)_3(SO_2)$ receives a larger *R* stabilization than $N(CH_3)_3(SO_2)$. This *R* interaction increases both the Ni sp orbital population and SO_2 electron population, but decreases the PH_3 electron population, as shown in Table IV, suggesting that *R* would be, in main character, the coupling between the Ni → SO_2 charge-transfer and the polarization (PH_3 → Ni electron transfer) of the $Ni(PH_3)_3$ part.[31] As depicted in Figure 3, $Ni(PH_3)_3$ has the accepting Ni 4s orbital (LUMO) at a lower energy level than the LUMO of $N(CH_3)_3$, and the d orbitals and PH_3 lone pairs of $Ni(PH_3)_3$ are slightly higher in energy than the lone pair and N–C p_σ bonding orbitals. This situation of orbital energies would result in a large polarization (PH_3 → Ni electron transfer) of $Ni(PH_3)_3$. Thus, the large *R* stabilization of $Ni(PH_3)_3(SO_2)$ would come from the presence of a low-lying unoccupied Ni 4s orbital. A comparison between $Ni(PH_3)_3(SO_2)$ and $N(CH_3)_3(SO)_2$ is briefly carried out for the η^1-coplanar structure; the former has larger ES, MSCTPLX, SMCTPLX, and *R* stabilization than the latter. This large ES stabilization would result from the electrostatic attraction between the SO_2 lone pair and the $Ni^{\delta+}$ atom. The large MSCTPLX stabilization comes from the high-lying occupied Ni d_{yz} orbital,

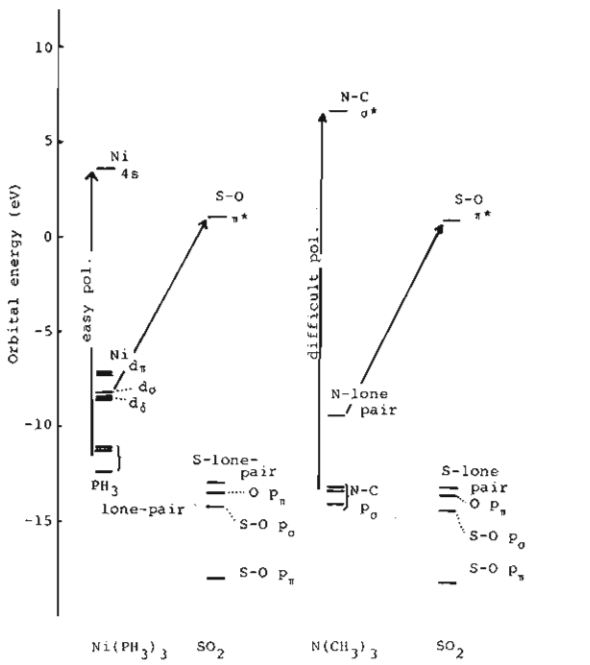

Figure 4. MO energies of $Ni(PH_3)_3$, $N(CH_3)_3$, and SO_2 near HOMO and LUMO. pol. represents polarization, and arrows indicate the electron transfer.

Chart IV

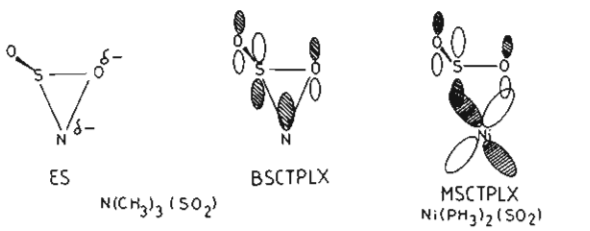

as has been discussed above, and the large SMCTPLX stabilization probably results from the presence of the unoccupied Ni 4s orbital at a relatively low-energy level (see Figure 3). The *R* stabilization would be considered to be the coupling between the SO_2 → Ni charge-transfer and the SO_2 and $Ni(PH_3)_3$ polarizations,[32] from the following electron distributions: (i) *R* decreases the S atomic population but increases the O atomic population; (ii) *R* decreases the SO_2 electron population (see Table IV). Thus, the larger *R* stabilization of η^1-coplanar $Ni(PH_3)_3(SO_2)$, including the SO_2 → Ni 4s charge transfer as an important component, would result from the low-lying unoccupied Ni 4s orbital, and the SO_2 coordinate bond of η^1-coplanar $Ni(PH_3)_3(SO_2)$ is characterized by the presence of a high-lying occupied Ni d_π orbital and the low-lying unoccupied Ni 4s orbital, compared with $N(CH_3)_3(SO_2)$. In conclusion, these comparisons about η^1-coplanar and η^1-pyramid structures suggest that the presence of a low-lying Ni 4s orbital, as well as the high-lying Ni d_π orbital and bulky PH_3 ligands, is considered to be one of the factors characterizing the Ni(0)–SO_2 complexes.

η^2-SO Coordination Mode. Comparison between $Ni(PH_3)_2(\eta^2\text{-}SO_2)$ and $N(CH_3)_3(\eta^2\text{-}SO_2)$. It is well-known that η^2-SO

(31) There is a possiblity that the *R* interaction is mainly contributed from the mutual charge transfer; one is the charge transfer from SO_2 to $Ni(PH_3)_3$ and another is the charge transfer from $Ni(PH_3)_3$ to SO_2. This mutual charge transfer is expected to little alter the SO_2 electron population. In the η^1-pyramid $Ni(PH_3)_3(SO_2)$, however, Mulliken population analysis of *R* shows that the SO_2 electron population is remarkably increased and the decrease in the Ni d_{z^2} orbital population corresponds to the increased electron population of SO_2. Further, the PH_3 electron population is decreased by the *R* interaction more largely than the by the MSCTPLX interaction. These electron distributions strongly suggest that the *R* interaction is the coupling between the charge transfer from $Ni(PH_3)_3$ to SO_2 and the polarization of $Ni(PH_3)_3$.

(32) *R* changes Mulliken populations of the $Ni(PH_3)_3$ part, similar to SMCTPLX, suggesting that *R* includes the SO_2 → Ni charge transfer and the $Ni(PH_3)_3$ polarization. *R* is also considered to include the SO_2 polarization, because neither SMCTPLX nor MSCTPLX decreases the S atomic population and simultaneously increases the O atomic population. Now, a comment is also given on the smaller *R* stabilization of the η^1-coplanar $Ni(PH_3)_3(SO_2)$ than that of the η^1-pyramid structure. The small *R* stabilization of the η^1-coplanar structure is probably due to the smaller decrease of symmetry by the SO_2 η^1-coplanar coordination than that by the SO_2 η^1-pyramid coordination. But, the *R* stabilization of the η^1-coplanar $Ni(PH_3)_3(SO_2)$ is much larger than that of the η^1-coplanar $N(CH_3)_3(SO_2)$, as shown in Table III.

Table V. Comparison of the Coordinate Bond between $Ni(PH_3)_2(\eta^2\text{-}SO_2)$ and $N(CH_3)_3(\eta^2\text{-}SO_2)$ (kcal/mol)

	$Ni(PH_3)_2(\eta^2\text{-}SO_2)$	$N(CH_3)_3(\eta^2\text{-}SO_2)$[a]
BE	−41.8	36.1
DEF[b]	15.5	0
INT	−57.3	36.1
ES	−91.4	−74.7
EX	159.6	159.6
MSCTPLX	−66.5	−27.9
SMCTPLX	−27.2	−16.6
R	−31.8	−4.3

[a] The distance between the N atom and the center of S=O double bond is taken to be 1.75 Å, giving the same EX value as that of $Ni(PH_3)_2(\eta^2\text{-}SO_2)$. [b] See footnote *d* of Table III.

coordination has not been found in any nonmetal SO_2 complex. In fact, the present MO calculation (3-21G) gives no binding energy (positive BE value) for $N(CH_3)_3(\eta^2\text{-}SO_2)$ (the ideal η^2-SO coordination structure, as described above), as shown in Figure 4; the total energy becomes lower and lower, when the SO_2 ligand moves from the η^2-SO coordination position toward the η^1-S coordination position, keeping the geometry and orientation of SO_2 fixed and keeping the coordinating S=O bond perpendicular to the C_{3v} axis of $N(CH_3)_3$. To make clear the reason, energy components are plotted in Figure 4 as functions of the above mentioned movement of SO_2. When we go from the η^2-SO coordination to the η^1-S coordination, the ES and BSCTPLX stabilizations are increased more than the increase in EX repulsion. These changes in ES and BSCTPLX are easily understood by considering electron distribution and overlap between the $N(CH_3)_3$ HOMO and the SO_2 LUMO (see Chart IV). Because N of $N(CH_3)_3$ and O of SO_2 are negatively charged, the η^2-SO coordination suffers from the N–O electrostatic repulsion but the η^1-pyramid structure hardly suffers from such electrostatic repulsion, yielding a large ES stabilization of the η^1-pyramid one. The BSCTPLX interaction is formed from the $N(CH_3)_3$ HOMO (lone pair) and the SO_2 LUMO (π^* orbital). Though these MO's hardly overlap with each other in the η^2-SO coordination structure (Chart IV), they can overlap well with each other in the η^1-pyramid coordination (Chart II), leading to large BSCTPLX stabilization of this structure. Consequently, the η^2-SO coordination disfavors BSCTPLX and ES interactions, which makes this structure unstable.

In contrast with nonmetal SO_2 complexes, a model complex of η^2-SO coordination, $Ni(PH_3)_2(SO_2)$, has a large negative BE value. A comparison between $Ni(PH_3)_2(\eta^2\text{-}SO_2)$ and $N(CH_3)_3(\eta^2\text{-}SO_2)$ is given in Table V, where $N(CH_3)_3(\eta^2\text{-}SO_2)$ is assumed to possess an ideal η^2-SO coordination structure (the N–SO_2 distance was taken to be 1.75 Å to give the same EX repulsion as that of $Ni(PH_3)_2(\eta^2\text{-}SO_2)$). Large differences in BSCTPLX and *R* interactions are found between these two complexes; $Ni(PH_3)_2(\eta^2\text{-}SO_2)$ receives much larger MSCTPLX and *R* stabilizations than $N(CH_3)_3(SO_2)$, which is the main factor making the η^2-SO coordinate $Ni(PH_3)_2(\eta^2\text{-}SO_2)$ stable. This strong MSCTPLX interaction would come from the high-lying Ni d_π orbital. As shown in Chart IV, the occupied Ni d_π orbital can interact well with the SO_2 π^* orbital in the η^2-SO coordination, to form a strong MSCTPLX interaction. The larger *R* stabilization would be due to the coupling of the Ni → SO_2 charge-transfer interaction with easy polarization of $Ni(PH_3)_2$, as has been described for $Ni(PH_3)_3(SO_2)$.[33]

In summary, the high-lying occupied d_π-orbital of Ni makes the η^2-SO coordination possible in $Ni(PH_3)_2(\eta^2\text{-}SO_2)$. Nonmetal Lewis bases do not have any such π-donor orbital interacting well with the SO_2 π^* orbital, and as a result, η^2-SO coordination is unstable.

Conclusions

In this work, ab initio MO studies were carried out on several nonmetal SO_2 complexes $N(CH_3)_3(SO_2)$, $(NH_3)(SO_2)$, $(CN^-)(SO_2)$, and $(NC^-)(SO_2)$ and Ni(0)–SO_2 complexes ($Ni(PH_3)_3(\eta^1\text{-}SO_2)$ and $Ni(PH_3)_2(\eta^2\text{-}SO_2)$). The optimized structures of examined complexes agree well with their experimental structures. All of the nonmetal SO_2 complexes examined have the η^1-pyramid structure, due to the lower EX repulsion and the larger charge-transfer interaction from Lewis base to SO_2. In the coplanar structure, the lone-pair orbital of the Lewis base overlaps well with the lone-pair orbital of SO_2, leading to the large EX destabilization. The lone pair of the Lewis base cannot overlap well with the SO_2 π^* orbital, not to form effective charge-transfer interaction with SO_2. Thus, nonmetal SO_2 complexes do not take the η^1-coplanar structure. In $Ni(PH_3)_3(SO_2)$, the situation is different from that of $N(CH_3)_3(SO_2)$. $Ni(PH_3)_3(SO_2)$ has bulky PH_3 ligands and a high-lying Ni d_π orbital. The η^1-pyramid structure is destabilized by the steric repulsion with bulky PH_3 ligands. On the other hand, the η^1-coplanar structure can receive moderate charge transfer from the Ni d_π to the SO_2 π^* orbital. As a result, $Ni(PH_3)_3(SO_2)$ takes the η^1-coplanar structure. The η^2-SO coordination mode is unstable in nonmetal SO_2 complexes, whereas this coordination seems possible in low-valent metal complexes. To make this coordination possible, the presence of a π-donor orbital is necessary. Though nonmetal Lewis bases do not have such a π-donor orbital, the occupied d_π orbital of $Ni(PH_3)_2$ can overlap well with the SO_2 π^* orbital to form a strong charge-transfer interaction from Ni to SO_2. In comparison with nonmetal SO_2 complexes, the characteristic features of Ni(0)–SO_2 complexes come from the presence of the high-lying occupied Ni d_π orbital, the low-lying unoccupied Ni 4s orbital, and bulky PH_3 ligands.

Acknowledgment. The authors thank Dr. K. Kitaura (Osaka City University) for his kind help in carrying out EDA calculations. This work was partially supported by the Joint Studies Program (1982–1983) of the Institute for Molecular Science (IMS). The numerical calculations were mainly carried out at the Computer Center of the IMS and partially at the Computer Center at Kyushu University.

Registry No. $N(CH_3)_3(SO_2)$, 31051-75-9; $(NH_3)(SO_2)$, 25310-87-6; $(CN^-)(SO_2)$, 98921-97-2; $(NC^-)(SO_2)$, 80475-45-2; $Ni(Ph_3)_3(SO_2)$, 98976-49-9; $Ni(PH_3)_2(SO_2)$, 98976-50-2.

(33) In $Ni(PH_3)_2(\eta^2\text{-}SO_2)$, *R* increases the SO_2 electron population and the Ni atomic population, but decreases the PH_3 electron population. These changes in Mulliken population suggest that *R* includes the coupling between the Ni → SO_2 charge transfer and the $Ni(PH_3)_3$ polarization (PH_3 → Ni), as is found in the η^1-pyramid $Ni(PH_3)_3(SO_2)$.